International Journal of Thermophysics, Vol. 17, No. 2, 1996

Numerical Simulation and Error Analysis for Thermal Diffusivity Measurements Using Laser-Induced Thermal Grating Technique

J. Wang,[1] M. Fiebig,[1,2] and G. Wu[3]

Received June 26, 1995

The laser-induced thermal grating technique has been used to determine the thermal diffusivity of liquids and liquid mixtures. But the dynamic behaviour of the transient thermal grating has not yet been thoroughly investigated, and the systematic errors, which result from the departures from one-dimensional heat conduction, have scarcely been studied quantitatively. In this paper, a three-dimensional numerical simulation and results of the transient thermal grating technique are presented, which enable a good understanding of the dynamic behaviour of the transient thermal grating. The results of this simulation are important for the proper design of the experimental setup to keep the systematic errors for the diffusivity measurement small. Based on the simulation method, the systematic errors were analyzed quantitatively. Here, the following effects were studied: (1) sample thickness, (2) intersection angle, (3) absorption, (4) Gaussian beam intensity distribution and focusing of heating laser beam, and (5) heating pulse duration and laser power. This error analysis makes it possible to specify the criteria for optimum measuring conditions, to correct the measured thermal-diffusivity values for systematic errors, and to estimate the accuracy of the measurements.

KEY WORDS: diffraction; forced Rayleigh scattering; laser-induced thermal grating, numerical simulation; thermal diffusivity, toluene.

1. INTRODUCTION

The laser-induced thermal grating technique has proved to be suitable for the determination of the thermal diffusivity of liquids and liquid mixtures

[1] Institut für Thermo- und Fluiddynamik, Ruhr-Universität Bochum, D-44780 Bochum, Germany.

[2] To whom correspondence should be addressed.

[3] National University of Singapore, Singapore.

0195-928X/96/0100-0329$09.50/0

[1–4]. Like other optical methods, this measurement technique has the advantage that measurements can be done without any physical contact between the sensor and the sample. Hence, it is suitable to employ this method when insertion of sensors is difficult, e.g., for the measurements of corrosive materials at high temperatures [5–7]. Because of the small temperature rise (typically smaller than 0.2 K) in the sample and the very short measuring time (below 4 ms), the influence of free convection is negligible. Moreover, only a very small sample volume (a few cubic millimeters) is required for the measurement, so that valuable materials can also be investigated.

Notwithstanding the advantages mentioned above, the dynamic behaviour of the transient thermal grating has not yet been thoroughly investigated. The systematic errors, which result from departures from one-dimensional heat conduction, have scarcely been studied quantitatively. There is only the work of Nagasaka et al. [2], in which the error factors are analyzed using Green's function and some assumptions are made. In this paper, a numerical simulation of the excitation and relaxation of the thermal grating is presented. The simulation results enable a good understanding of the dynamic behavior of the transient thermal grating. On the basis of this method, an appropriate error analysis for the thermal-diffusivity measurements with the transient thermal grating technique was carried out and is presented in this paper. The following error effects were studied in this work: (1) sample thickness, (2) intersection angle, (3) absorption, (4) Gaussian beam intensity distribution and focusing of the heating laser beam, and (5) heating pulse duration and laser power. This error analysis can be used to specify the experimental conditions under which some of the systematic error effects can be nearly compensated and provides the theoretical basis for correcting measured thermal-diffusivity values. The accuracy of the measurements can thus be improved and the remaining error can be estimated.

2. MATHEMATICAL MODEL

The principle of the laser-induced thermal grating technique has been described by Eichler et al. [1], Nagasaka et al. [2], and Wu et al. [3]. The basic theory is based on one-dimensional heat conduction model which is valid, if the grating constant Λ is much smaller than the sample thickness d, and the diameter of the heated region d_h and d are much smaller compared to the absorption length of the sample α^{-1} (see Fig. 1). Consequently, the induced periodic temperature distribution, which is produced

by interference of two laser beams of equal wavelength λ_h during the heating period ($0 < t \leqslant t_h$), decays exponentially with the relaxation time

$$\tau_c = \frac{1}{a}\left(\frac{\Lambda}{2\pi}\right)^2 \tag{1}$$

after the heating process ($t > t_h$).

Due to the spatially periodic temperature distribution, a corresponding refractive index distribution is produced, which acts as an optical phase grating. This transient grating can be probed with a third laser beam of wavelength λ_p. According to the diffraction theory [8], the thermal diffusivity of the sample can be determined by detecting the time dependence of the first-order diffracted probing beam $I_1(t)$

$$I_1(t) \propto \exp(-2t/\tau_c) \tag{2}$$

and

$$a = (\tau_c q^2)^{-1} \tag{3}$$

where $q = 2\pi/\Lambda = (2\pi/\lambda_h)\sin\theta$, and θ is the intersection angle of the heating beams.

Under real experimental conditions, systematic deviations from Eq. (2) occur because the heat conduction is not strictly one-dimensional. In this work, we simulate numerically the excitation and relaxation processes of the thermal grating with a three-dimensional heat-conduction model and calculate the diffracted intensity by using the classical scattering theory. From this, we can acquire a good understanding of the dynamic behavior of the transient thermal grating. The error analysis can also be carried out with this numerical method.

The full description of the excitation and relaxation of the transient thermal grating is provided by the unsteady three-dimensional Fourier-equation (Fig. 1)

$$\frac{\partial T(\mathbf{r}, t)}{\partial t} = a\,\nabla^2 T(\mathbf{r}, t) + \frac{\alpha I(x, y, t)}{\rho c_p} \tag{4}$$

$$\frac{\partial T_m(\mathbf{r}, t)}{\partial t} = a\,\nabla^2 T_m(\mathbf{r}, t) + \frac{\alpha I_m(x, y, t)}{\rho c_p} \tag{5}$$

where the total and the average intensities of the heating beam I and I_m are

$$I(x, y, t) = \begin{cases} 2I_0 e^{-2(x^2+y^2)/w^2}[1+\cos(qx)] & 0 < t \leqslant t_h \\ 0 & t > t_h \end{cases}$$

$$I_m(x, y, t) = \begin{cases} 2I_0 e^{-2(x^2+y^2)/w^2} & 0 < t \leqslant t_h \\ 0 & t > t_h \end{cases}$$

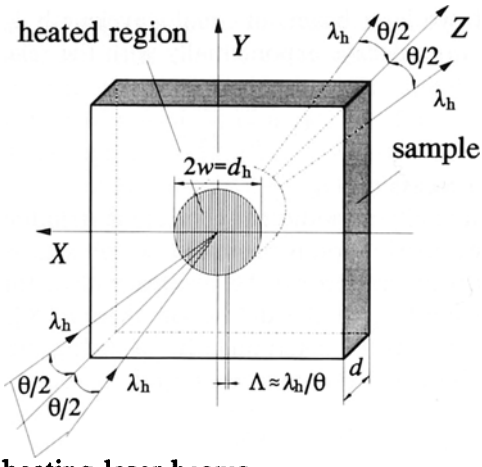

Fig. 1. Schematic of the sample and heated region.

In the equations above, T is the temperature, T_m the average temperature, α the absorption coefficient, I_0 the intensity of each heating beam, $2w$ the diameter of the heated region, q the modulus of the grating vector, and t_h pulse duration of heating. $\mathbf{r}$ and t have the usual meaning of spacial coordinate vector and time. a, ρ, and c_p stand for the thermal diffusivity, the density, and the heat capacity of the sample, respectively.

Consider one excitation–relaxation period of the transient thermal grating. We get the initial conditions

$$T(\mathbf{r}, 0) = T_0 \tag{6}$$

$$T_m(\mathbf{r}, 0) = T_0 \tag{7}$$

and the boundary conditions

$$\frac{\partial T(\mathbf{r}, t)}{\partial x} = 0, \qquad \frac{\partial T_m(\mathbf{r}, t)}{\partial x} = 0, \qquad x = 0 \tag{8}$$

$$T(\mathbf{r}, t) = T_0, \qquad T_m(\mathbf{r}, t) = T_0, \qquad |x| \gg 2w \tag{9}$$

$$\frac{\partial T(\mathbf{r}, t)}{\partial y} = 0, \qquad \frac{\partial T_m(\mathbf{r}, t)}{\partial y} = 0, \qquad y = 0 \tag{10}$$

$$T(\mathbf{r}, t) = T_0, \qquad T_m(\mathbf{r}, t) = T_0, \qquad |y| \gg 2w \tag{11}$$

and

$$T(\mathbf{r}, t) = T_0 + \frac{2q(t)_{z=0}}{b_1 + b_2}\sqrt{\frac{t}{\pi}}, \qquad z = 0 \tag{12}$$

$$T_m(\mathbf{r}, t) = T_0 + \frac{2q_m(t)_{z=0}}{b_1 + b_2}\sqrt{\frac{t}{\pi}}, \qquad z = 0 \tag{13}$$

$$T(\mathbf{r}, t) = T_0 + \frac{2q(t)_{z=d}}{b_1 + b_2}\sqrt{\frac{t}{\pi}}, \qquad z = d \tag{14}$$

$$T_m(\mathbf{r}, t) = T_0 + \frac{2q_m(t)_{z=d}}{b_1 + b_2}\sqrt{\frac{t}{\pi}}, \qquad z = d \tag{15}$$

where T_0 is the initial temperature, d the sample thickness, b_1 and b_2 the heat-penetration depths of the sample material, and the glass windows ($b = \rho c_p a^{1/2}$), and $q(t)$, and $q_m(t)$ are the local heat fluxes on the boundary between the sample material and the glass windows, which are related to the temperature gradients of T and T_m through the Fourier equation $\mathbf{q} = -\lambda \nabla T$[9].

By solving Eqs. (4) and (5) for given experimental conditions (d, θ, w, α, I_0, t_h) and the properties of the sample (a, c_p, ρ), the temperature fluctuations $\delta T(\mathbf{r}, t)$ can be determined (Fig. 2)

$$\delta T(\mathbf{r}, t) = T(\mathbf{r}, t) - T_m(\mathbf{r}, t) \tag{16}$$

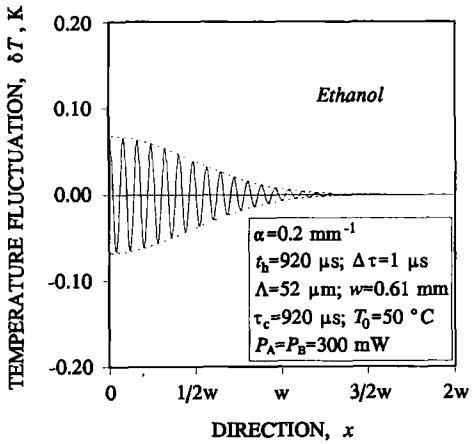

Fig. 2. Temperature fluctuations δT in the modulation direction of the thermal grating—simulation on ethanol.

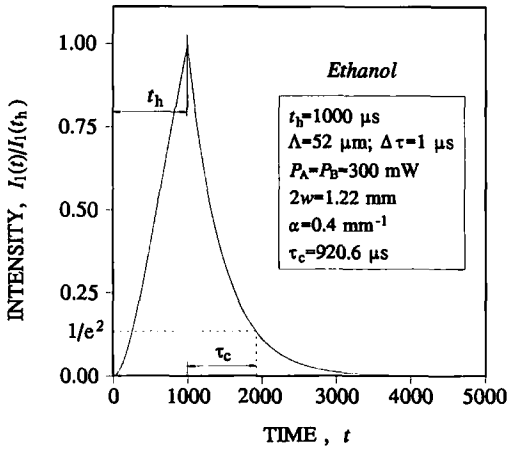

Fig. 3. Diffracted intensity I_1 in the excitation and relaxation phases of the thermal grating—simulation on ethanol.

The spatial Fourier transformation of $\delta T(\mathbf{r}, t)$ gives the time dependence of the first-order diffracted intensity (Fig. 3) according to the classical scattering theory [3, 10]

$$I_1(t) \propto \left[\int e^{i\mathbf{q}\cdot r}\, \delta T(\mathbf{r}, t)\, d\mathbf{r} \right]^2 \tag{17}$$

The relaxation time τ_c can be evaluated by fitting the calculated data from Eq. (17) into the exponential function as shown in Eq. (2) and we get a new thermal diffusivity a' from Eq. (3), which is called an apparent property. By comparing the value a' with the previously given thermal-diffusivity value a of the sample, the systematic error can be determined.

3. DYNAMIC BEHAVIOR OF TRANSIENT THERMAL GRATINGS

The dynamic behavior of the transient thermal grating is very important for the understanding of its excitation and relaxation processes and also for the correct setting of the experimental conditions.

Figure 4 shows the simulated temperature distributions in the modulation direction of the heating beams for selected times during and immediately after the light pulse. At the beginning of the excitation process, the temperature field is fully modulated and a grating structure is gradually formed. At the same time, an increasingly larger background of average temperature rise is produced due to the increasingly larger temperature difference between the grating peaks and the valleys. After the light pulse, the

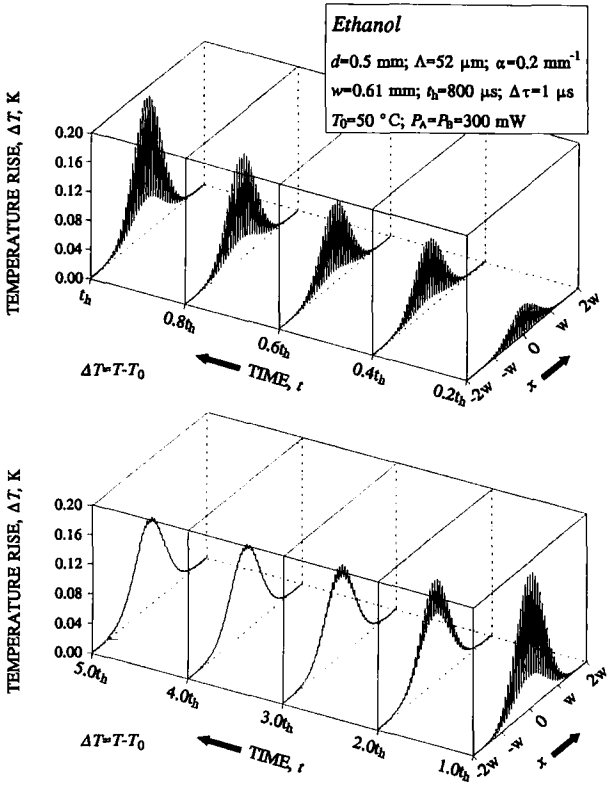

Fig. 4. Development of the temperature distributions in x-direction during and immediately after a light pulse—simulation on ethanol.

grating structure decays exponentially. From Fig. 4 we can see that the temperature grating has disappeared at $t = 4t_h \sim 5t_h$.

Compared with the grating structure, the average temperture rise decays thousands of times slower (Fig. 5). Thus it can be seen that the heating pulse repetition rate has to be kept small enough to avoid an excessive temperature rise in the heating region. This should be fulfilled by a good experimental setup.

Because of the Gaussian intensity distribution of the heating laser beam (TEM_{00} mode), a Gaussian temperature distribution in y-direction is produced during the heating period, which decays also thousands of times slower than the grating structure. It should be noted that heat leaks to the unheated regions in x- and y-directions ($|x| > 2w$, $|y| > 2w$) due to the Gaussian temperature distributions, which may lead to a systematic error. This error effect will be discussed in Section 4.4 of this paper.

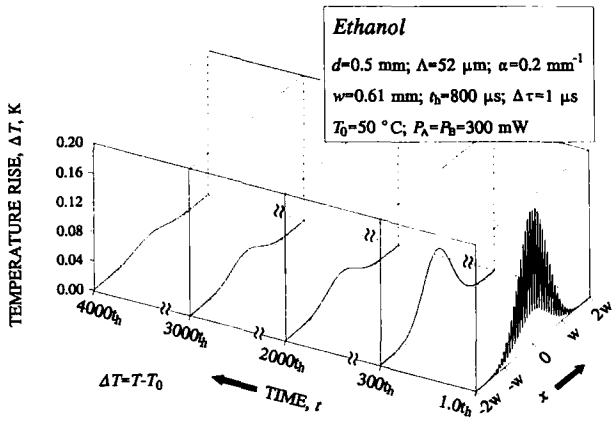

Fig. 5. Development of the temperature distributions in x-direction after a light pulse with large relaxation time—simulation on ethanol.

During the heating period, a temperature distribution is formed in z-direction with the lapse of time. This temperature distribution is characterized by high temperatures due to heat conduction near both glass windows (Fig. 6). In the middle of the sample, the temperature is kept nearly constant in z-direction for a very weak absorption. The heat conduction at both boundary surfaces results in a systematic error, which must be corrected in the measurement and is also discussed in Section 4.1 of this paper. With an increasingly larger absorption coefficient, a temperature

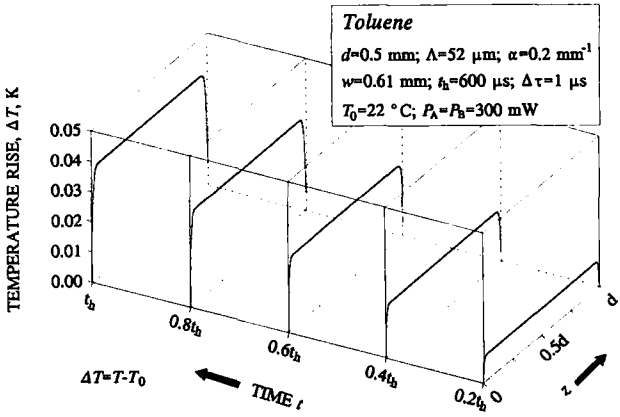

Fig. 6. Development of the temperature distributions in z-direction during the heating period—simulation on toluene.

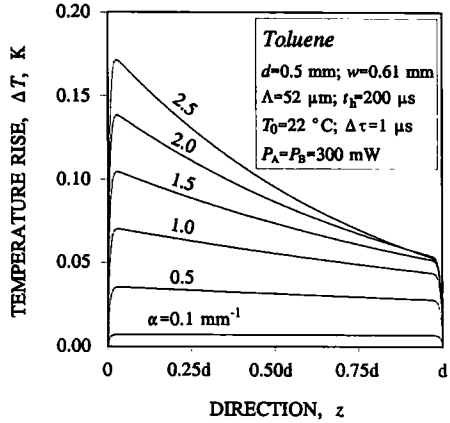

Fig. 7. Dependence of temperature distribution in z-direction on absorption coefficient.

gradient in the bulk of the sample will be generated (Fig. 7). This temperature distribution causes heat conduction in z-direction in the sample and leads to an error (effect of absorption).

4. ERROR ANALYSIS

By using the simulation method stated in Section 2, the systematic effects of sample thickness, intersection angle, absorption coefficient, Gaussian beam intensity distribution and focusing of heating laser beams, and heating pulse duration and laser power can be numerically analyzed.

4.1. Effect of Sample Thickness

The error due to the sample thickness $\Delta a/a = (a' - a)/a$ can be obtained by simulating the excitation and relaxation of the thermal grating, where a' is the apparent thermal diffusivity and a the given value used in the simulation. Figure 8 shows the dependence of the error $\Delta a/a$ on the ratio between the grating constant and the sample thickness Λ/d and on the thermophysical properties of the sample. In this work, the glass windows are assumed to be Pyrex glass with given thermophysical properties, and the simulation results for three liquids, water, toluene, and refrigerant R123, are presented, which have very different thermal-diffusivity values. From Fig. 8, it can be seen that the dependence of the error $\Delta a/a$ on the thermophysical properties of the sample is small. Even at a large Λ/d, e.g.,

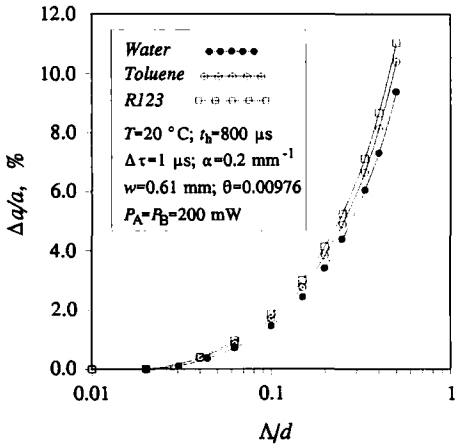

Fig. 8. Effect of sample thickness in terms of ratio Λ/d: simulation at 20°C; α, absorption coefficient; t_h, heating pulse length; $\Delta\tau$, sample time; w, spot size of heating beams; P_A and P_B, power of heating beams; θ, intersection angle.

$\Lambda/d = 0.2$, the difference of $\Delta a/a$ between water and R123 is only 0.7%. At $\Lambda/d < 0.04$, $\Delta a/a$ is smaller than 0.5%. But its effect should be taken into account when making corrections for systematic errors to experimental results.

The calculated values for $\Delta a/a$ in this work were found to be lower than the results obtained by Nagasaka et al. using Green's function [2]. At $\Lambda/d = 0.1$, for example, the difference between both calculated values for $\Delta a/a$ is ca. 0.75% for water and 0.9% for toluene.

4.2. Effect of Intersection Angle

Usually, measurements are carried out with given sample thickness d (typically 0.5 mm), and the grating constant Λ can be changed by adjusting the intersection angle θ

$$\Lambda = \frac{\lambda_h}{2\sin(\theta/2)} \approx \frac{\lambda_h}{\theta}, \qquad \theta \approx 0 \tag{18}$$

It is thus very meaningful to study the effect of the intersection angle θ at the given sample thickness d.

When the sample thickness d, the absorption coefficient α, the radius w of the heating beams, etc., are kept constant, and only the intersection

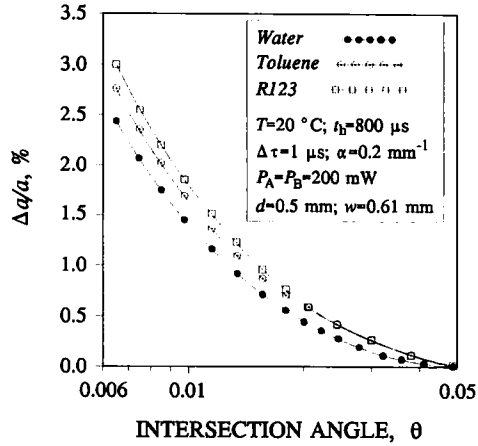

Fig. 9. Effect of intersection angle in terms of θ: simulation at 20°C; α, absorption coefficient; t_h, heating pulse length; $\Delta\tau$, sample time; d, sample thickness; w, spot size of heating beams; P_A and P_B, power of heating beams.

angle of both heating beams θ varies, the error $\Delta a/a$ decreases with increasing the intersection angle as shown in Fig. 9. Because the sample thickness d is usually given (typically 0.5 mm) and the intersection angle θ can be adjusted to a certain value in experiments, Fig. 9 provides the basis for correcting the systematic error.

4.3. Effect of Absorption

A suitable absorption of the heating beams is necessary for the excitation of the thermal grating. By doping with a very small amount of a dye, the absorption coefficient α of the sample can be significantly increased. It is usually possible to keep the concentration of the dye in the sample so low that the addition of the dye does not exert any influence on the thermophysical properties of the sample. However, a temperature distribution in z-direction (see Figs. 1 and 7), which is proportional to the absorption coefficient α of the sample, will be generated through absorption of the heating power. Due to this temperature distribution, the unsteady one-dimensional heat conduction model is no longer valid.

The effect of absorption coefficient α is shown in Fig. 10. In the calculation, a large sample thickness d is chosen to meet the condition $d > \alpha^{-1}$, so that the effect of sample thickness can be neglected, and only the influence of the absorption coefficient on the measurements is con-

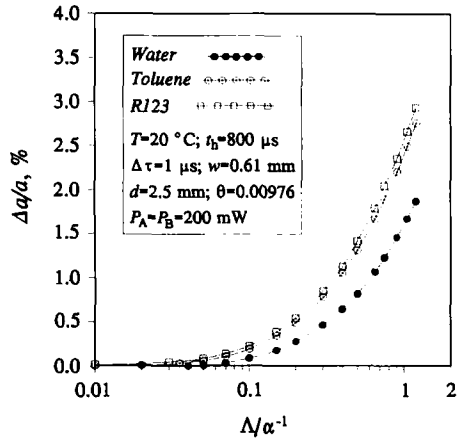

Fig. 10. Effect of absorption in terms of Λ/α: simulation at 20°C; d, sample thickness; t_h, heating pulse length; $\Delta\tau$, sample time; w, spot size of heating beams; P_A and P_B, power of heating beams; θ, intersection angle.

sidered here. The results for toluene and R123 are in good agreement with those obtained by Nagasaka et al. [2]. At $\Lambda/\alpha^{-1} = 0.4$, for example, our results are very similar to those from Ref. 2 (ca. 0.05% difference for toluene and 0.15% for R123). However, our results for water are lower in comparison, and at $\Lambda/\alpha^{-1} = 0.4$, the calculated value for $\Delta a/a$ differs from that by Nagasaka by ca. 0.4%.

As shown in Fig. 10, the effect of absorption coefficient α can be neglected, when $\Lambda/\alpha^{-1} < 0.05$. In practice, it is usually possible to keep the absorption coefficient α of the sample so small that the absorption is sufficient for the measurements, but the effect of α can still be neglected.

4.4. Effect of Gaussian Beam Intensity Distribution and Focusing

In the basic theory, it is assumed that the laser beams, which generate the thermal grating, possess an uniform intensity distribution. Consequently, a temperature grating structure with a constant amplitude in the infinite area of the sample will be produced. In the measurements, the heating laser beams of TEM_{00} mode have a Gaussian intensity distribution with a spot size w (at intensity $1/e^2 \approx 14\%$). Thus, we obtain a superposition of the Gaussian temperature distribution on the grating structure, which causes heat loss to the unheated region in the sample. Moreover, the heating and probing beams are usually focused in the experiments to inten-

sify the diffracted signal and improve the signal-to-noise ratio significantly [3, 4]. As a result, the spot size of the laser beam is reduced. Here, the effects of reduction of the laser beam diameter due to focusing and Gaussian beam intensity distribution will be discussed together.

According to the calculations, the effect of Gaussian beam intensity distribution and focusing of heating laser beams causes a reduction in the measured apparent thermal diffusivity ($\Delta a < 0$), as shown in Fig. 11. This implies that the superposition of the Gaussian temperature distribution on the grating structure delays the relaxation of the thermal grating. Taking the focusing of the laser beams into consideration in the calculation, we define a parameter $f^*(0 < f^* \leqslant 1)$, so that we get the actual diameter of the heating beams $d = 2w = f^* \cdot 2w_0$, where d_0 and w_0 are the diameter and the radius of the unfocused heating beams. In general, we can choose the parameters f^* and Λ in experiments to meet the condition $\Lambda/(f^* \cdot w) < 0.1$ (see Fig. 11), so that the effect of Gaussian beam intensity distribution and focusing can be neglected.

In this analysis, we have calculated the time dependence of the first-order diffracted intensity by means of the spacial Fourier transformation of the temperature fluctuations $\delta T(\mathbf{r}, t)$. For this reason, the intensity distribution of the probing beam could not be taken into consideration here.

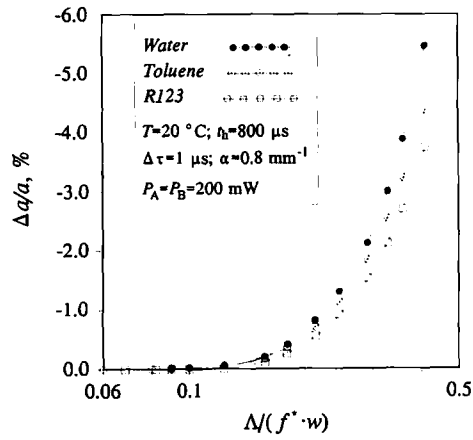

Fig. 11. Effect of Gaussian beam intensity distribution and focusing of heating laser beams in terms of $\Lambda/(f^* \cdot w)$: simulation at 20°C; α, absorption coefficient; t_h, heating pulse length; $\Delta\tau$, sample time; P_A and P_B, power of heating beams.

4.5. Effect of Heating Pulse Duration and Laser Power

From Eq. (17) we know that the intensity of the first-order diffracted signal I_1 is proportional to the spuare of the temperature fluctuation δT, viz., the initial temperature amplitude ΔT_0

$$I_1(t) \propto \delta T^2 \propto \Delta T_0^2 \tag{19}$$

To generate a sufficiently large intial temperature amplitude, more precisely, an adequate signal-to-noise ratio, we can either extend the heating pulse duration time t_h or enhance the heating laser power P, when the absorption coefficient α of the sample is kept constant. However, an excessively extended heating pulse duration time t_h leads possibly to the distortion of the temperature distribution as a result of heat loss through the glass windows during the excitation of the grating.

Calculations show that the error due to the effect of heating pulse duration time and heating laser power is smaller than 0.01%, even with a very long heating pulse duration (e.g., $t_h = 2000\ \mu s$). Thus, we come to the conclusion that the effect of heating pulse duration and heating laser power on the measurements is negligible. However, with increasing of t_h or P the temperature rise in the sample will be possibly increased to an unacceptable value. As an example, the dependence of the maximum temperature rise in the sample toluene ΔT_{max} on the heating pulse duration time t_h and power of both heating laser beams $P_A = P_B = P/2$ is presented in Fig. 12. It gives a reference to the heating during the excitation of the thermal grating in measurements.

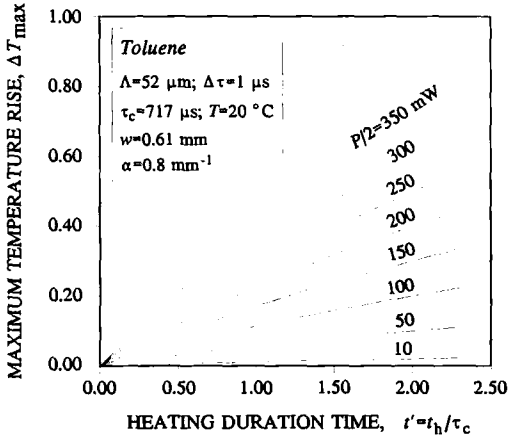

Fig. 12. Maximum temperature rise ΔT_{max} in terms of heating duration time t_h and heating laser power $P_A = P_B = P/2$.

5. EXPERIMENTAL EXAMPLE AND ERROR ESTIMATION

As an example, the thermal diffusivity of toluene has been measured with the laser-induced thermal grating technique. The experimental setup is simular to that used by Wu et al. [3]. The unique differences lies in employing a shutter behind the chopper, which allows to change the heating pulse repetition rate [4]. Thus, the repetition rate can be kept small enough to avoid an excessive temperature rise in the heated region. In the experiment, the sample was doped with methyl red. The absorption coefficient was measured to be about 0.8 mm^{-1}.

Figure 13 shows the measured thermal diffusivity of toluene at room temperature as a function of intersection angle included between both heating beams. Obviously, the measured thermal diffusivity increases with decreasing intersection angle θ and parameter Q, which is defined to describe the effect of grating thickness [2, 8]

$$Q=\frac{2\pi\, d\lambda_p}{\Lambda^2 n} \tag{20}$$

where λ_p denotes the wevelength of the probing beam, and n is the refractive index of the sample.

Based on the numerical error analysis, we can estimate the total systematic error with the given sample thickness $d=0.5$ mm (sum of the effects of intersection angle, absorption, and Gaussian beam intensity dis-

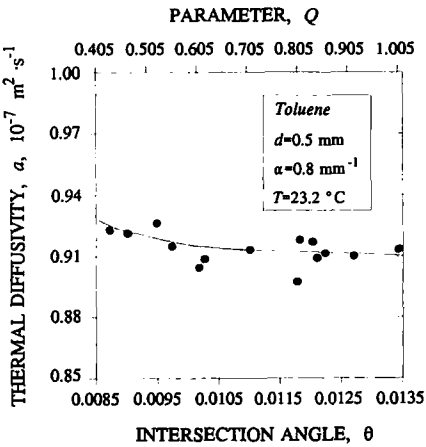

Fig. 13. Measured thermal diffusivity of toluene in terms of intersection angle θ and parameter Q.

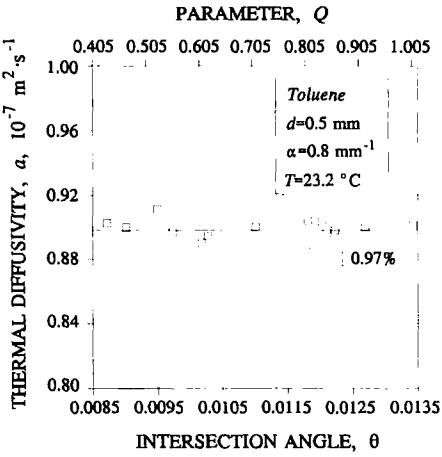

Fig. 14. Thermal diffusivity of toluene in terms of intersection angle θ and parameter Q after error correction.

tribution and focusing of heating laser beam) and make corrections to the measured thermal diffusivity. The thermal-diffusivity values after correcting are shown in Fig. 14. We see that they become independent of the intersection angle θ and parameter Q with an average value of $0.898 \times 10^{-7} m^2 \cdot s^{-1}$. The result agrees very good with the data obtained by Hendrix et al. [11] (1.8%) and by Knibbe and Raal [12] (1.1%). The modulus q of the grating vector can be measured to an accuracy of 0.55%. The determination of the relaxation time τ_c of the first-order diffracted intensity is accurate to within $\pm 1\%$. Therefore, the overall accuracy of the present measurements is estimated to be $\pm 1.5\%$.

6. CONCLUSIONS

In this paper, a numerical simulation of the excitation and the relaxation of the transient thermal grating were presented, which enables us a good understanding of the dynamic behaviour of the transient thermal grating. This simulation method has been applied to analyze the systematic errors for the thermal-diffudivity measurements. This error analysis can be used to give the experimental conditions under which some of the systematic error effects can be compensated and provides the theoretical basis for the correction of measured thermal-diffusivity values. The accuracy of the measurements can thus be improved and the remaining error can be estimated. The experimental example shows that the results of the thermal diffusivity for toluene at atmospheric temperature after correction to the measured values agree very good with the reference data.

ACKNOWLEDGMENTS

The authors gratefully acknowledge the financial support of the *Deutsche Forschungsgemeinschaft (DFG)* and the *Deutsche Forschungsanstalt für Luft- und Raumfahrt e.V. (DLR).*

REFERENCES

1. H. Eichler, G. Salje, and H. Stahl, *J. Appl. Phys.* **44**:5383 (1973).
2. Y. Nagasaka, T. Hatakeyama, M. Okuda, and A. Nagashima, *Rev. Sci. Instrum.* **59**:1156 (1988)
3. G. Wu, M. Fiebig, and J. Wang, *Fluid Phase Equil.* **88**:239 (1993)
4. J. Wang and M. Fiebig, *Int. J. Thermophys.* **16**:1353 (1995).
5. Y. Nagasaka and A. Nagashima, *Int. J. Thermophys.* **9**:923 (1988).
6. N. Nakazawa, M. Akabori, Y. Nagasaka, and A. Nagashima, *Trans. JSME* **B56**:1467 (1990).
7. Y. Nagasaka, N. Nakazawa, and A. Nagashima, *Int. J. Thermophys.* **13**:555 (1992).
8. H. J. Eichler, P. Günter, and D. W. Pohl, *Laser-Induced Dynamic Gratings* (Springer-Verlag, Berlin, 1986), p. 98.
9. J. Wang, *Dr.-Thesis* (Ruhr-Universität Bochum, 1994).
10. B. J. Berne and R. Pecora, *Dynamic Light Scattering* (John Willey & Sons, New York, 1976), p. 26.
11. M. Hendrix, A. Leipertz, M. Fiebig, and G. Simonsohn, *Int. J. Heat Mass Transfer* **33**:333 (1987).
12. G. Knibbe and J. D. Raal, *Int. J. Thermophys.* **8**:181 (1987).